arXiv:1607.06991v2 [physics.optics] 20 Dec 2016

Large static tuning of narrow-beam terahertz plasmonic lasers operating at 78 K

Chongzhao Wu,[1] Yuan Jin,[1] John L. Reno,[2] and Sushil Kumar[1,*]

[1] *Department of Electrical and Computer Engineering, Lehigh University, Bethlehem, PA 18015, USA*

[2] *Sandia National Laboratories, Center of Integrated Nanotechnologies, MS 1303, Albuquerque, NM 87185, USA*

Abstract

A new tuning mechanism is demonstrated for single-mode metal-clad plasmonic lasers, in which refractive-index of the laser's surrounding medium affects the resonant-cavity mode in the same vein as refractive-index of gain medium inside the cavity. Reversible, continuous, and mode-hop-free tuning of ~ 57 GHz is realized for single-mode narrow-beam terahertz plasmonic quantum-cascade lasers (QCLs), which is demonstrated at much more practical temperature of 78 K. The tuning is based on post-process deposition/etching of a dielectric (Silicon-dioxide) on a QCL chip that has already been soldered and wire-bonded onto a copper mount. This is a considerably larger tuning range compared to previously reported results for terahertz QCLs with directional far-field radiation patterns. The key enabling mechanism for tuning is a recently developed antenna-feedback scheme for plasmonic lasers, which leads to generation of hybrid surface-plasmon-polaritons propagating outside the cavity of the laser with a large spatial extent. The effect of dielectric deposition on QCL's characteristics is investigated in detail including that on maximum operating temperature, peak output power and far-field radiation patterns. Single-lobed beam with low divergence ($< 7^\circ$) is maintained through the tuning range. The antenna-feedback scheme is ideally suited for modulation of plasmonic lasers and their sensing applications due to the sensitive dependence of spectral and radiative properties of the laser on its surrounding medium.

* Email: sushil@lehigh.edu

INTRODUCTION

Plasmonic lasers that utilize metal-clad cavities confine electromagnetic energy in the form of surface-plasmon-polaritons (SPPs) at subwavelength dimensions. They have seen rapid development for targeted applications in nanoscale optics and integrated optical sensing. The most common types of plasmonic lasers utilize Fabry-Pérot type cavities in which one dimension is not subwavelength and is typically much longer than the other two dimensions [1–3]. For applications requiring spectral purity (single-mode operation) at the desired wavelength, tunability is a desired characteristic that is challenging to implement for such lasers. This stems from the difficulty in external control of the resonant-cavity mode such as that in conventional external-cavity tuning techniques for semiconductor lasers, since the subwavelength characteristics of such lasers lead to poor coupling between the cavity-modes with free-space propagating modes. Prior work on development of tunable plasmonic lasers has primarily focused on changing the gain medium of the cavity itself [4, 5]. Terahertz quantum-cascade lasers (QCLs) [6–8] with metallic cavities [9] are one such subset of plasmonic lasers, which also suffer for such challenges with respect to their tunability.

Terahertz QCLs are the brightest available solid-state sources [10] of coherent terahertz radiation. They have witnessed significant development in the past decade in multiple areas such as wave engineering with distributed-feedback (DFB) techniques [11], output-power [12], temperature performance, frequency-coverage [13–15], and frequency tunability [16]. Single-mode terahertz QCLs are particularly required for a multitude of applications in sensing and spectroscopy. However, due to limits on accuracy of lithography utilized to implement DFB, it is still challenging to achieve single-mode emission from DFB QCLs at the exact desired frequency for applications such as high-resolution heterodyne spectroscopy [17, 18]. Frequency tuning post-fabrication is desired to overcome this problem. Up to now, a variety of tuning techniques for terahertz QCLs have been demonstrated. Temperature tuning is simple but lacks large tunability [19]. Techniques such as applying external-cavities [20, 21] or modal perturbation using electromechanical methods [22–24] have the ability to achieve large tuning range but at the cost of discontinuous tuning, or system complexity and poor radiation patterns and temperature performance for such QCLs respectively.

A static-tuning technique based on post-process dielectric deposition was recently demon-

strated for terahertz QCLs with third-order DFB operating at $\sim$ 10 K with a tuning of $\sim$ 5 GHz [25]. (The tuning could be extended while the QCL is in operation, but only temporarily, by deposition of solid nitrogen through multiple-cycle condensation to $\sim$ 25 GHz in a liquid-Helium cryostat). Along similar lines, we here demonstrate a greatly enhanced continuous tuning range of $\sim$ 57 GHz for single-mode QCLs emitting at 2.8 THz and operating at 78 K, achieved by deposition of Silicon-dioxide post-fabrication, and with significantly improved beam profiles. Prior work on large ($>$ 20 GHz) tuning in Refs. [22, 23, and 25] is achieved by perturbing the lateral evanescent mode of metallic cavities, which requires the cavities to be made very narrow (deep-subwavelength, $\lesssim$ 10 μm wide cavities with the standard 10 μm thickness), and thereby makes the fabrication very challenging (with the requirement of sophisticated dry-etching techniques) as well as degrades the temperature and power performance of the QCLs considerably. In contrast, the tuning in this report places no such restrictions on the dimensions of the QCL cavity and is demonstrated for wide cavities processed with routine wet-etching methods. The large tuning is facilitated by a recently developed "antenna-feedback" scheme for plasmonic lasers, which was experimentally implemented for terahertz QCLs with metallic cavities [26]. This mode-hop free tuning performance can be controlled by the thickness of deposited Silicon-dioxide, is reversible, and can be implemented on already mounted and soldered QCL chips, which makes it attractive for future commercialization of single-mode terahertz QCLs. Importantly, in contrast to all previous tuning results for terahertz QCLs that have been demonstrated at temperatures close-to that of liquid-Helium, this work achieves large tuning for QCLs operating in a liquid-Nitrogen cooled dewar since the tuning mechanism does not impact the gain of the QCL sensitively. Neither does the tuning method mandate a large dynamic range in current for the QCL in operation, which is in contrast with the methods relying on frequency-pulling due to Stark-shifted gain spectrum with changing electrical bias of the QCL that requires operation at low-temperatures [27–29].

DESCRIPTION OF THE TUNING TECHNIQUE

Plasmonic lasers, of which the terahertz QCLs with metallic cavities are a specific example, lead to highly divergent far-field radiation patterns owing to the subwavelength dimensions of their radiating apertures. The antenna-feedback scheme for plasmonic lasers [26]

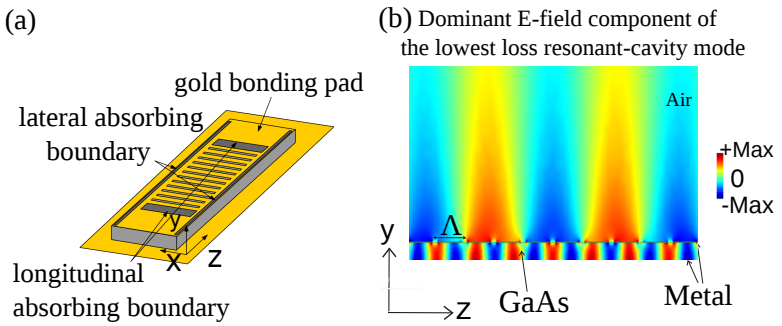

FIG. 1. (a) Schematic of a terahertz plasmonic laser cavity with the antenna-feedback scheme. A parallel-plate metallic cavity is shown with slit-like apertures in its top metal cladding with a specific periodicity Λ as determined from equation (1), which lead to coupling of a guided SPP wave inside the cavity (interacting with the gain medium) with a single-sided SPP wave with a large spatial extent in the surrounding medium. The lateral and longitudinal absorbing boundaries are implemented to selectively excite the lowest order lateral and longitudinal resonant-cavity modes respectively. (b) The dominant electric-field component (E_y) of the lowest-loss resonant-cavity mode is plotted along z axis, computed with finite-element (FEM) simulations using a commercial software package (Comsol 4.3). The height of the cavity is 10 μm. A hybrid SPP mode is excited in the surrounding medium that is phase-locked to a guided SPP mode inside the cavity.

couples the resonant surface-plasmon-polariton (SPP) mode in the cavity to a highly directional far-field radiation pattern. This occurs by exciting hybrid SPPs with a large spatial extent in the surrounding medium of the cavity by the mechanism of Bragg diffraction, which is affected by implementation of a grating in the metal-cladding of the plasmonic laser as illustrated in Fig. 1(a). With the choice of a specific periodicity in the grating, the resonant SPP wave inside the cavity is coupled via distributed-feedback (DFB) to a hybrid SPP wave that can propagate in the surrounding medium on the opposite side of the metal-film being used in the cavity of the plasmonic laser.

For terahertz QCLs with metallic cavities the antenna-feedback scheme could be implemented by introducing slit-like-apertures in its top metallic cladding as shown schematically in Fig. 1(b). For a chosen grating periodicity Λ, a DFB mode with free-space wavelength λ (and frequency $\nu = c/\lambda$) given by the equation

$$\lambda = (n_c + n_s)\,\Lambda \tag{1}$$

is resonantly excited for the case when the coupling between the SPP wave in the cavity and the SPP wave in the surrounding medium is via first-order Bragg diffraction [26]. Here, n_c is the effective propagation index of the SPP wave inside the cavity (which is approximately

same as the refractive-index of the cavity's active medium) and n_s is the effective propagation index of the hybrid SPP wave in the surrounding medium (which is approximately same as the refractive-index of the surrounding medium).

Equation (1) is distinctly different from that of any other solid-state DFB lasers that has been reported in literature, in that the refractive index of the surrounding medium is equally important in setting the resonant-frequency of the DFB mode of the laser as is the refractive index of the active medium inside the cavity. In other conventional solid-state lasers, the effect of the surrounding medium on the resonant-frequency is primarily a function of the fraction of evanescent mode of the cavity that propagates in its surroundings (typically represented by a mode-confinement factor, Γ), which is also the case for the tunable terahertz QCL reported in Ref. 25. However, in the antenna-feedback scheme, the contribution of the surrounding medium is due to considerations of phase-matching [26] rather than the fraction of the overall electromagnetic energy propagating outside the cavity. Consequently, the resonant-frequency of the DFB mode depends sensitively on the refractive-index of the surrounding medium that could be altered to tune the frequency of the plasmonic laser, which is the technique employed for terahertz QCLs presented here. To the best of our knowledge, this is a unique mechanism to tune the frequency of a solid-state laser for which there is no analogous precedent in literature.

A 10 μm thick terahertz QCL structure was grown by molecular beam epitaxy with a three-well resonant-phonon GaAs/$Al_{0.10}Ga_{0.90}As$ design scheme [30]. The metallic QCL cavities with antenna-feedback gratings were fabricated using standard wafer-wafer thermo-compression bonding and contact lithography technique. Fig. 1(b) shows a 2D finite-element (FEM) simulation of the dominant TM-polarized (E_y) electric-field for a typical cavity (of infinite-width, for 2D simulation) with antenna-feedback gratings in the top-metal cladding. As can be seen, the the resonant DFB mode excites a single-sided SPP wave in the surrounding medium, which is established as a standing-wave on the top-metal cladding with a large spatial extent in the vertical dimension (y direction). Hence, any changes in the refractive index of the surrounding medium serve to change the effective propagation constant n_s of the single-sided SPP mode, which tunes the excitation frequency of the resonant-DFB mode according to equation (1).

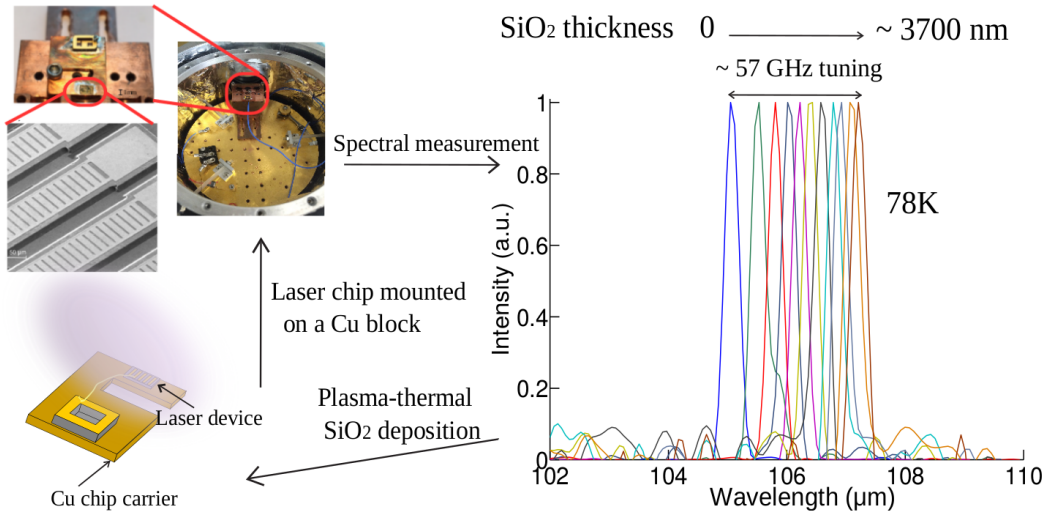

FIG. 2. Optical image of a mounted QCL semiconductor chip out of which one of the QCLs with the antenna-feedback scheme is wire-bonded for electrical characterization. The QCL chip is soldered on a small copper chip that itself is screwed onto a bigger copper heat-sink to be mounted on the cold-plate of a cryogenic dewar. Multiple rounds of Silicon-dioxide deposition and cryogenic measurements were performed on the soldered and mounted QCL chip using PECVD. The tuning of the QCL's single-mode lasing spectrum is shown as a function of the thickness of the deposited oxide. Spectra were measured after each deposition step when the QCL was operated in a liquid-Nitrogen cooled dewar at 78 K in pulsed mode at an operating current of $\sim$ 570 mA (current-density $\sim$ 405 A/cm^2). A net tuning of $\sim$ 57 GHz tuning is demonstrated for an overall deposited thickness of $\sim$ 3700 nm.

RESULTS

The active-medium of the QCLs is based on a three-well resonant-phonon design with GaAs/$Al_{0.10}Ga_{0.90}$As superlattice (design RTRP3W197, wafer number VB0464), which is described in Ref. [30], and was grown by molecular-beam epitaxy. The QCL superlattice is 10 μm thick with an average n-doping of 5.5×10^{15} cm^{-3}, and surrounded by 0.05 μm and 0.1 μm thick highly-doped GaAs contact layers at 5×10^{18} cm^{-3} on either side of the superlattice. Fabrication of QCLs with parallel-plate metallic cavities followed a Cu-Cu thermocompression wafer bonding technique as in Ref. [19] with standard optical contact lithography. Lateral and longitudinal absorbing boundaries were implemented by exposing the highly doped GaAs layer in the finally fabricated cavities, and the fabrication procedure is the same as in Ref. 26. Ti/Au metal layers of thickness 25/200 nm were used as the top metal cladding, using an image-reversal lithography mask for implementing gratings in the metal layers. Another positive-resist lithography step was used to cover the grating-

metal with photoresist to be used as a mask for wet-etching of ridges in a H_2SO_4:H_2O_2:H_2O 1:8:80 solution. A Ti/Au contact was used as the backside-metal contact for the finally fabricated QCL chips to assist in soldering. Before deposition of backside-metal of the wafer, the substrate was mechanically polished down to a thickness of ~ 170 μm to improve heat-sinking.

By deposition of Silicon-dioxide post-fabrication (after the QCL chip is already mounted and wire-bonded on a copper mount), the lasing frequency of the resonant antenna-feedback mode is tuned sensitively. Fig. 2 shows the variation of a specific QCL's wavelength of emission when increasing the thickness of blanket deposited Silicon-dioxide on the entire QCL chip. As expected from equation (1), the lasing wavelength undergoes a red-shift with increasing thickness of the oxide, since then, the effective propagation index n_s for the SPP wave in the surrounding medium of the QCL will increase. Additional details about changes to the hybrid SPP mode, and correspondingly n_s, with oxide deposition are provided in supplementary material (section S1). The measured QCL has a grating period $\Lambda = 25$ μm and the cavity's dimensions are 100 μm $\times$ 1.4 mm $\times$ 10 μm. A cleaved chip consisting of QCLs with antenna-feedback gratings was In-soldered on a Cu block, the QCL to be tested was wire-bonded for electrical biasing, and the Cu block was mounted on the cold-stage of a liquid Nitrogen vacuum cryostat for measurements. In this experiment, the frequency of the QCL was first measured without any dielectric deposition, and it radiated in a single-mode at $\sim$ 2.85 THz ($\lambda \sim 105$ μm). Afterwards, the resonant-frequency is changed by depositing Silicon-dioxide on top of the mounted QCL chip using a plasma-enhanced chemical vapor deposition (PECVD) system. The deposited thickness is carefully calibrated by simultaneously including a bare GaAs wafer in the PECVD chamber for each deposition step. QCL's spectra were measured at 78 K in linear-scan mode with a resolution of 0.2 cm^{-1} using a FTIR with room-temperature pyroelectric detector. Multiple cycles of spectral measurement and oxide-deposition were implemented and the tuning results are collected and shown in Fig. 2, which illustrates a large red-shift tuning with this mechanism. Finally, a mode-hop-free and continuous tuning of $\sim$ 57 GHz was achieved after an overall deposited thickness of $\sim$ 3700 nm. Further tuning could not be realized since QCL stopped lasing at 78 K beyond the stated thickness. The spectra shown in Fig. 2 were all measured at similar bias currents. When etching away the deposited SiO_2 on top of the laser device by buffered-HF (BOE 7 : 1) etchant, the QCL was characterized again and its emission

properties including the lasing wavelength returned to its original value, which illustrates that tuning by post-process deposition of SiO_2 on terahertz QCLs here is a reversible method.

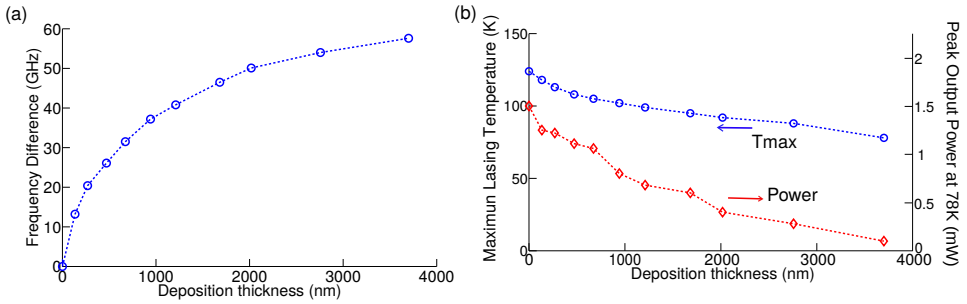

FIG. 3. (a) Emission frequency of the terahertz QCL with antenna-feedback as a function of the deposited thickness of Silicon-dioxide, expressed as a difference from its original emission frequency of ~ 2.85 THz without any oxide. The QCL is biased slightly below the peak-power bias region where it radiates in a single-mode (detailed spectra with bias are shown in Fig. 4). (b) Maximum operating temperature ($T_{\max}$) and the detected peak optical power at 78 K for the QCL in pulsed operation, as a function of the thickness of the Silicon-dioxide.

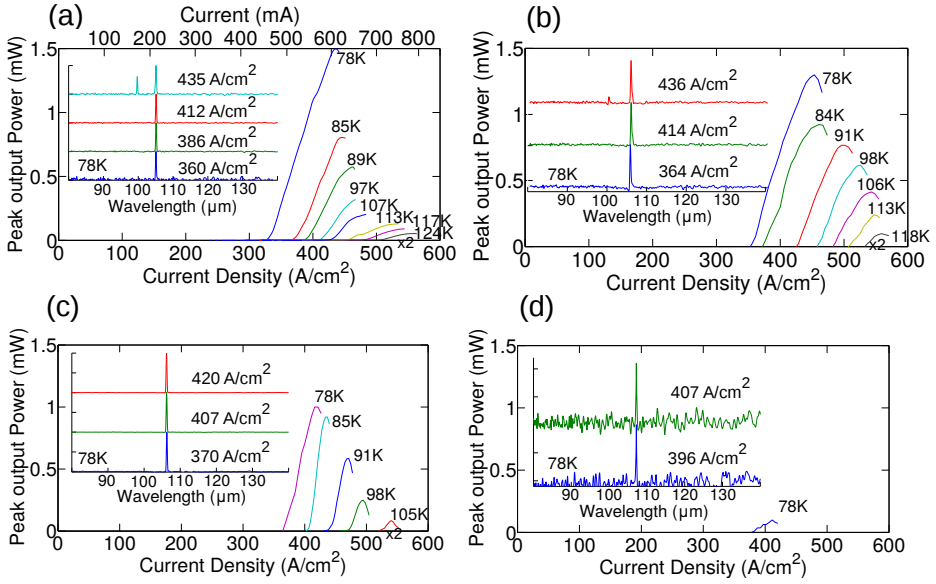

FIG. 4. Light-current characteristics of the terahertz QCL with antenna-feedback scheme at different heat-sink temperatures. The dimensions of the QCL's cavity are 100 μm$\times$1.4 mm$\times$10 μm. The QCL is biased in pulsed mode with 400 ns wide pulses repeated at 100 kHz. The plot-insets show lasing spectra at 78 K as a function of increasing bias. (a) Original QCL without any oxide deposition, (b) QCL with 140 nm thick oxide leading to $\sim$ 13 GHz frequency tuning, (c) QCL with 700 nm thick oxide leading to $\sim$ 31 GHz frequency tuning, and (d) QCL with 3700 nm thick oxide leading to the maximum tuning of $\sim$ 57 GHz for the QCL still lasing at 78 K.

Figure 3(a) characterizes the variation of the QCL's emission frequency as a function of thickness of the deposited Silicon-dioxide. The variation is non-linear, and the rate of tuning

as a function of oxide-thickness decreases as more oxide is deposited. A 2D finite-element simulation was not able to reproduce this non-linear tuning since the hybrid SPP mode in the surrounding medium of the cavity in the vertical direction (above the cavity) has a large spatial extent. Correspondingly, the tuning computed with 2D simulations is predominantly linear for an overall oxide thickness of few microns. However, it is argued that the non-linear tuning behavior as observed here is due to the complex spatial nature of the SPP mode in the surrounding medium in the lateral dimensions [26], which is difficult to capture even with 3D simulation due to hardware limitations in performing such simulations. The experimental tuning result is compared to that predicted from both 2D and 3D simulations in the supplementary material (section S2). The dependency of measured maximum lasing temperature and peak output power at 78 K with oxide thickness is shown in Figure 3(b). Without any post-process deposition of the oxide, this terahertz QCL device lased up to 124 K with peak output-power of $\sim$ 1.5 mW at 78 K. When deposition thickness reaches $\sim$ 3700 nm and $\sim$ 57 GHz tuning is obtained, the maximum lasing temperature of this device is slightly above 78 K and the peak output-power reduces to $\sim$ 100 uW at 78 K. The emitted optical power was measured with a deuterated triglycine sulfate pyroelectric detector (DTGS) pyroelectric detector (Gentec THz 2I-BL-BNC) and calibrated with a terahertz thermopile power-meter (ScienTech model AC2500H) without any optical component or cone collecting optic inside the cryostat. The power values are reported without any corrections to the detected signal.

Two reasons contribute to the decrease in maximum lasing temperature and output-power of the QCL with increasing oxide thickness. First, thin-film oxide deposited by PECVD is a lossy material at terahertz frequencies for which the absorption coefficient could be as high as 20 cm^{-1} [31]. Secondly, the confinement factor Γ of the resonant-cavity mode, which is the fraction of the mode that resides in the active-medium, decreases as thicker oxide is deposited. This is primarily because the higher electric-permittivity of the oxide $\epsilon_{\text{ox}} \sim 4.4\epsilon_0$ (at terahertz frequencies). As a consequence the effective threshold gain is increased for exciting the resonant-cavity mode, which also reduces optical power due to an increase in the effective modal propagation loss in the cavity as well as reduction in the net dynamic range for lasing current. A precise analytical or numerical estimation of the net effect of oxide thickness on the threshold gain and QCL's temperature and power performance is beyond the scope of this work because, first, in case of terahertz QCLs various transport

parameters as well as waveguide loss parameters cannot be predicted accurately, and second, the estimation of Γ requires 3D finite-element simulation of the QCL's cavity with deposited oxide that cannot be done due to aforementioned reasons.

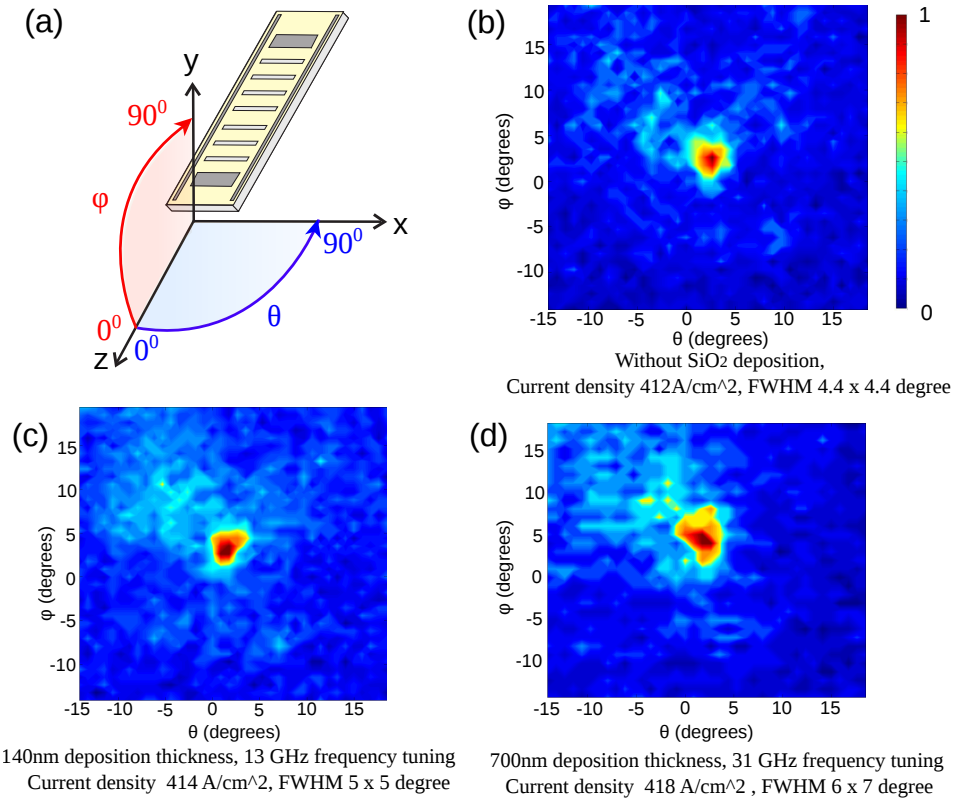

FIG. 5. (a) Schematic showing orientation of the QCL and definition of angles for the shown far-field radiation patterns. The QCL was operated at 78 K in pulsed mode, and the radiation pattern was measured using a room-temperature pyroelectric detector of 2 mm diameter mounted on a $x-y$ movement stage. The radiation-pattern in (b) is for QCL without Silicon-dioxide deposition, in (c) is for QCL deposited with an oxide thickness of 140 nm, and in (d) is for an oxide thickness of 700 nm.

Figure 4 shows light-current (L-I) characteristics in pulsed operation for the QCL operated at different heat-sink temperatures along with its lasing spectra at different bias when varying deposition thickness of the Silicon-dioxide. The QCL predominantly radiates at a single frequency around 2.84 THz that corresponds to the desired DFB mode of the cavity. However, at higher current-densities closer to peak operating bias (> 420 A/cm^2), a second mode at shorter-wavelength is excited, which suggests that a higher-order lateral mode was likely excited due to spatial-hole burning in the cavity (since such a mode has a smaller effective propagation index n_c in the cavity). The excitation of the higher-order lateral mode ceases in the entire operating range of the QCL as thicker oxide is deposited. When

the oxide thickness is increased to $\sim$ 700 nm corresponding to $\sim$ 31 GHz frequency tuning, the QCL lased up to 105 K with peak output-power of $\sim$ 1 mW at 78 K. Single mode spectra with lasing frequency $\sim$ 2.82 THz were measured under all bias conditions over the whole dynamic range, namely from threshold until negative differential-resistance (NDR) as shown in Figure 4(c). When total thickness of the deposited oxide is $\sim$ 3700 nm, only limited spectra were recorded at current-densities of $\sim$ 396 A/cm^2 and $\sim$ 407 A/cm^2 respectively while the QCL is still operating at 78 K in a liquid-Nitrogen cooled dewar. The QCL stopped lasing at 78 K when additional oxide was deposited. The threshold current-densities at 78 K for the aforementioned plots as shown in Fig. 4 are $\sim$ 328 A/cm^2, $\sim$ 350 A/cm^2, $\sim$ 364 A/cm^2, $\sim$ 390 A/cm^2 respectively, which increase with the thickness of the deposited oxide. From the data presented in Fig. 3 and Fig. 4 it can be noted that more than 60 % of the available tuning (i. e. $\sim$ 35 GHz tuning) could be realized by depositing less than 1 μm thick Silicon-dioxide, in which case there is no significant degradation in maximum operating temperature or power output from the QCL.

Radiation in a directional (narrow) beam is one of the most important and attractive characteristics of terahertz plasmonic QCLs with the antenna-feedback scheme [26]. Figure 5 shows measured beam patterns of the QCL at 78 K for varying thicknesses of the deposited oxide. Far-field radiation patterns were measured with a DTGS pyroelectric cell detector mounted on a computer-controlled two-axis moving stage in the end-fire (z) direction at a distance of 65 mm from the QCL's end-facets. Without any oxide, the QCL emits in a single-lobed beam with narrow divergence with full-width half-maximum (FWHM) of $\sim 4.4^\circ \times 4.4^\circ$ as shown in Fig. 5(b). After 140 nm thick oxide was deposited, the radiation pattern remained single-lobed but with a slightly increased FWHM of $\sim 5^\circ \times 5^\circ$. A further deposition of oxide to a thickness of 700 nm increased the FWHM of the main lobe to $\sim 6^\circ \times 7^\circ$. The small increase in beam divergence for thicker oxide deposition is likely due to reduction in spatial extent of the SPP mode on top of the cavity with oxide thickness. Due to the limits in the sensitivity of the of the room-temperature DTGS detector, the radiation patterns could not be measured with a reasonable signal-to-noise ratio after deposition of even thicker oxide. However, since the QCL continues to radiate in the same cavity mode, it should retain its characteristic radiation into single-lobed narrow beams.

DISCUSSION

Plasmonic lasers utilize metallic cavities to confine the electromagnetic mode at sub-wavelength dimensions. However, poor radiative coupling to free-space makes it difficult to statically or dynamically tune their emission frequency, which is required for practical applications. The tuning mechanisms demonstrated so-far involve alteration of gain-medium itself. Terahertz QCLs with metallic cavities suffer from similar challenges that has prevented development of tunable QCLs that could work at high-temperatures. In this work, we show that a recently developed antenna-feedback scheme for plasmonic lasers could offer an ideal solution for both static tuning (as demonstrated here) or dynamic tuning and frequency modulation (in principle, which is discussed further in section S3 of the supplementary material), while simultaneously achieving single-mode operation and narrow-beam emission from the sub-wavelength plasmonic cavities. The antenna-feedback scheme leads to the establishment of a hybrid SPP standing-wave in the surrounding medium of the laser's cavity with a large spatial extent. The emission frequency of the plasmonic laser depends sensitively on the effective propagation index of the SPP mode in the surrounding medium, which could be altered independently of the gain medium used inside the laser's cavity. Consequently small perturbations in the refractive-index of the surrounding medium could lead to large modulation in the laser's emission frequency. To the best of our knowledge, this is a unique mechanism to tune the frequency of a solid-state laser for which there is no analogous precedent in prior literature.

For terahertz QCLs, the antenna-feedback scheme was implemented for wide cavities that could operate well above the temperature of liquid-Nitrogen, in contrast with previous tuning techniques that have mostly utilized ultra-narrow cavities for access to the evanescent cavity modes. 57 GHz static tuning is demonstrated for single-mode narrow-beam terahertz QCLs emitting at 2.8 THz, based on post-process deposition of Silicon-dioxide on an already soldered and mounted QCL chip. A beam divergence of $< 7^{\circ}$ was maintained through the tuning range. The degradation of maximum operating-temperature and power output is small for a large fraction of the tuning range. More than 50 % of the available tuning ($\sim$ 30 GHz tuning) could be realized by depositing ~ 0.7 μm thick Silicon-dioxide, in which case $T_{\max}$ reduces from 124 K to 105 K and the peak output-power reduces from 1.5 mW to 1 mW. The tuning is reversible and continuous, and could pave the way for future commer-

cialization of DFB terahertz QCLs for targeted applications in sensing and high-resolution spectroscopy. Whereas all previous tuning results for terahertz QCLs were demonstrated at operating temperatures close to that of liquid-Helium, the results presented here are for QCLs operating at the much more practical temperature of 78 K, while simultaneously achieving significantly more directional beams compared to previous reports.

ACKNOWLEDGMENTS

This work is supported by the United States National Science Foundation through grants ECCS 1351142 and CMMI 1437168. The work is performed, in part, at the Center for Integrated Nanotechnologies, a U.S. Department of Energy (DOE), Office of Basic Energy Sciences user facility. Sandia National Laboratories is a multiprogram laboratory managed and operated by Sandia Corporation, a wholly owned subsidiary of Lockheed Martin Corporation, for the U.S. DOEs National Nuclear Security Administration under contract DE-AC04-94AL85000.

SUPPLEMENTAL DOCUMENTS

See supplementary material for discussions about the effective propagation index of the hybrid SPP wave in the surrounding medium, finite-element simulations of the tuning behavior, and a proposed dynamic tuning scheme.

---

[1] M. T. Hill, M. Marell, E. S. P. Leong, B. Smalbrugge, Y. Zhu, M. Sun, P. J. van Veldhoven, E. J. Geluk, F. Karouta, Y.-S. Oei, R. Nötzel, C.-Z. Ning, and M. K. Smit, Opt. Express **17**, 11107 (2009).

[2] R. F. Oulton, V. J. Sorger, T. Zentgraf, R.-M. Ma, C. Gladden, L. Dai, G. Bartal, and X. Zhang, Nature **461**, 629 (2009).

[3] Y.-J. Lu, J. Kim, H.-Y. Chen, C. Wu, N. Dabidian, C. E. Sanders, C.-Y. Wang, M.-Y. Lu, B.-H. Li, X. Qiu, W.-H. Chang, L.-J. Chen, G. Shvets, C.-K. Shih, and S. Gwo, Science **337**, 450 (2012).

[4] Y.-J. Lu, C.-Y. Wang, J. Kim, H.-Y. Chen, M.-Y. Lu, Y.-C. Chen, W.-H. Chang, L.-J. Chen, M. I. Stockman, C.-K. Shih, and S. Gwo, Nano Lett. **14**, 4381 (2014).

[5] A. Yang, T. B. Hoang, M. Dridi, C. Deeb, M. H. Mikkelsen, G. C. Schatz, and T. W. Odom, Nature Comm. **6**, 6939 (2015).

[6] R. Köhler, A. Tredicucci, F. Beltram, H. E. Beere, E. H. Linfield, A. G. Davies, D. A. Ritchie, R. C. Iotti, and F. Rossi, Nature **417**, 156 (2002).

[7] B. S. Williams, Nature Photonics **1**, 517 (2007).

[8] M. S. Vitiello, G. Scalari, B. Williams, and P. D. Natale, Opt. Express **23**, 5167 (2015).

[9] B. S. Williams, S. Kumar, H. Callebaut, Q. Hu, and J. L. Reno, Appl. Phys. Lett. **83**, 2124 (2003).

[10] G. Chattopadhyay, IEEE Trans. THz Sci. Technol. **1**, 33 (2011).

[11] C. Sirtori, S. Barbieri, and R. Collombelli, Nat. Photon. **7**, 691 (2013).

[12] L. Li, L. Chen, J. Zhu, J. Freeman, P. Dean, A. Valavanis, A. G. Davies, and E. H. Linfield, Electron. Lett. **50**, 309 (2014).

[13] G. Scalari, C. Walther, M. Fischer, R. Terazzi, H. Beere, D. Ritchie, and J. Faist, Laser Photonics Rev. **3**, 45 (2009).

[14] S. Kumar, IEEE J. Sel. Topics Quantum Electron. **17**, 38 (2011).

[15] S. Fathololoumi, E. Dupont, C. W. I. Chan, Z. R. Wasilewski, S. R. Laframboise, D. Ban, A. Mátyás, C. Jirauschek, Q. Hu, and H. C. Liu, Opt. Express **20**, 3866 (2012).

[16] M. S. Vitiello and A. Tredicucci, IEEE Trans. THz Sci. Technol. **1**, 76 (2011).

[17] Y. Ren, J. N. Hovenier, R. Higgins, J. R. Gao, T. M. Klapwijk, S. C. Shi, B. Klein, T.-Y. Kao, Q. Hu, and J. L. Reno, Appl. Phys. Lett. **98**, 231109 (2011).

[18] H.-W. Hübers, R. Eichholz, S. G. Pavlov, and H. Richter, J. Infrared Milli. Terahz. Waves **34**, 325 (2013).

[19] S. Kumar, B. S. Williams, Q. Qin, A. W. M. Lee, Q. Hu, and J. L. Reno, Opt. Express **15**, 113 (2007).

[20] J. Xu, J. M. Hensley, D. B. Fenner, R. P. Green, L. Mahler, A. Tredicucci, M. G. Allen, F. Beltram, H. E. Beere, and D. A. Ritchie, Appl. Phys. Lett. **91**, 121104 (2007).

[21] A. W. M. Lee, B. S. Williams, S. Kumar, Q. Hu, and J. L. Reno, Opt. Lett. **35**, 910 (2010).

[22] Q. Qin, J. L. Reno, and Q. Hu, Opt. Lett. **36**, 692 (2011).

[23] N. Han, A. de Geofroy, D. P. Burghoff, C. W. I. Chan, A. W. M. Lee, J. L. Reno, and Q. Hu, Opt. Lett. **39**, 3480 (2014).

[24] F. Castellano, V. Bianchi, L. Li, J. Zhu, A. Tredicucci, E. H. Linfield, A. G. Davies, and M. S. Vitiello, Appl. Phys. Lett. **107**, 261108 (2015).

[25] D. Turčinková, M. I. Amanti, F. Castellano, M. Beck, and J. Faist, Appl. Phys. Lett. **102**, 181113 (2013).

[26] C. Wu, S. Khanal, J. L. Reno, and S. Kumar, Optica **3**, 734 (2016).

[27] H. Zhang, L. A. Dunbar, G. Scalari, R. Houdré, and J. Faist, Opt. Express **15**, 16818 (2007).

[28] L. A. Dunbar, R. Houdré, G. Scalari, L. Sirigu, M. Giovannini, and J. Faist, Appl. Phys. Lett. **90**, 141114 (2007).

[29] D. Turčinková, M. I. Amanti, G. Scalari, M. Beck, and J. Faist, Appl. Phys. Lett. **106**, 131107 (2015).

[30] S. Khanal, L. Zhao, J. L. Reno, and S. Kumar, J. Opt **16**, 094001 (2014).

[31] K.-S. Lee, T.-M. Lu, and X.-C. Zhang, IEEE Circuits and Dev. Mag. **18**, 23 (2002).

Large static tuning of narrow-beam terahertz plasmonic lasers operating at 78 K

Chongzhao Wu, Yuan Jin, John L. Reno and Sushil Kumar

Supplementary Information

I. EFFECTIVE PROPAGATION INDEX OF THE HYBRID SPP MODE

The wavelength selected by antenna-feedback scheme is $\lambda = \Lambda(n_c + n_s)$ as shown in Ref. [26], which is different from all previously reported $p - th$ order distributed-feedback (DFB) schemes in which the DFB mode occurs at $\lambda = 2n_c\Lambda/p$. Here, n_s is an "effective" propagation index for the hybrid SPP wave propagating in the surrounding medium of the cavity that is bound to the top metallic cladding. It plays characteristic role in determining the resonant frequency of DFB mode and its tunability, since the wavelength of the resonant-cavity mode depends sensitively on n_s. It is beyond the scope of this work to describe the spatial profile of the electric-field corresponding to the surrounding SPP wave analytically, even for the relatively simple case when no SiO_2 is present. In the following, the profile of the SPP wave is computed numerically via finite-element simulations. As expected, n_s is closer to that of SiO_2 as the thickness of SiO_2 is increased, since a larger fraction of the SPP wave will then exist in SiO_2 instead of air (vacuum).

Fig. 6(a) shows the absolute value of electric-field, $|E|$, both inside the cavity and above the metal cladding for the antenna-feedback scheme from a 2D simulation (i.e. for a cavity with 'infinite' lateral width). The layer sequence includes an active region of 10 μm thickness and top metal cladding of 400 nm thickness that is modeled as lossless metal. The sub-wavelength plasmonic resonant optical mode inside the cavity is phased-locked with a hybrid SPP mode that travels on top of the metal cladding outside the cavity as mentioned in the main text. The SPP wave is relative tightly bound to the top metal cladding and decays (somewhat) exponentially in the length of the order of the wavelength in the surrounding material/medium. Attributed to the fact that the decay length in metal is negligible and independent of the loss in metal or thickness in metal (which was verified independently via

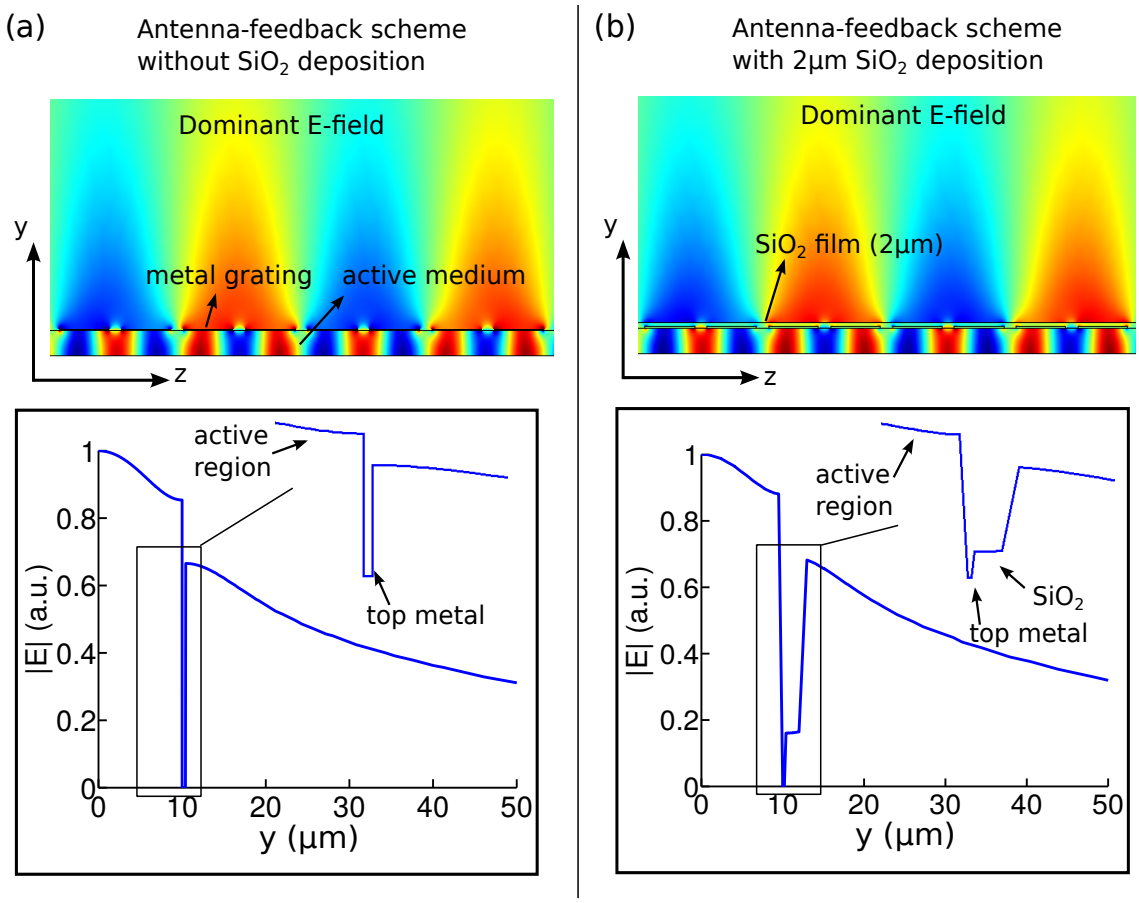

FIG. 6. **Comparison of the electric-field profile of the resonant-cavity mode with and without SiO_2 deposition** (a) Magnitude of the electric-field $|E|$ for the lowest-loss resonant-cavity mode computed by 2D finite-element simulations. The 10 μm thick GaAs cavity has antenna-feedback gratings in its top metal cladding. The mode-confinement factor for the active-region is ~ 70 %. (b) Electric-field profile for the same cavity but now with a 2 μm thick SiO_2 layer added on top of the cavity. In this case, ~ 1 % of the mode's energy is confined in the SiO_2 layer, which is approximately 4 % of the energy in the hybrid SPP wave outside the cavity/active-region.

finite element simulations with lossy metal), it is possible to qualitatively estimate the effect of SiO_2 film on the effective refractive index n_s of single-side SPP mode that propagates on the top of the cavity.

Fig. 6(b) shows the simulation result for a specific example in which the deposited SiO_2 film is 2 μm thick on the top of the laser cavity. The electric-energy stored in SiO_2 layer is computed to be ~ 4 % of the total energy in the SPP wave in the surrounding medium of the cavity, which leads to the effective n_s becoming ~ 1.045 $(= 0.04n_{\text{oxide}} + 0.96n_{\text{air}})$ calculated by the weighted contributions from SiO_2 and vacuum according to the fraction of confined energy in the respective medium (where the refractive index of SiO_2 is taken

as $n_{\mathrm{oxide}} \sim 2.1$ at terahertz frequencies). This provides a general idea about the change in resonant-frequency of the DFB mode, since from eq. (1) in the main text,

$$-\frac{d\nu}{\nu} = \frac{d\lambda}{\lambda} = \frac{dn_{\mathrm{s}}}{n_{\mathrm{s}}}\left(\frac{n_{\mathrm{s}}}{n_{\mathrm{c}} + n_{\mathrm{s}}}\right)$$

An increase in n_{s} by ~ 4.5 % should lead to a decrease of resonant frequency by ~ 1 % according to the expression above, which is indeed observed from the simulated results for the resonant-frequency of the DFB mode. This verifies the validity of eq. (1) from the main text and the fact that n_{s} is an effective propagation index of the hybrid SPP wave. However, note that the analysis based on 2D simulations will not provide an accurate estimate of the effective index n_{s} for real experiments. The SPP wave in the surrounding medium extends significantly in the lateral directions beyond the width of the cavity as described in Ref. [26], and hence attains a complex 3D profile. Even small variations in the geometry of the cavity (including the angle of the sidewalls and the distance to the neighboring cavities) affects the shape of the hybrid SPP wave, and correspondingly the resonant-frequency of the DFB mode. Hence, the simplistic 2D finite-element simulations could be utilized to understand the modal behavior only qualitatively.

II. FINITE-ELEMENT SIMULATION OF TUNING CHARACTERISTICS

A comparison between simulated and experimental tuning curves as a function of the thickness of deposited oxide is shown in Fig. 7. The tuning computed with 2D simulations is predominantly linear for an overall oxide thickness of few microns. However, it is argued that the non-linear tuning behavior as observed in experiments is due to the complex spatial nature of the hybrid SPP mode in the surrounding medium for cavities with finite width, which was also discussed in Ref. [26]. The modal behavior can only be captured partially by 3D simulations due to limitations in accuracy of the modeled geometry as well as memory limitations for finite-element simulations that require the absorbing boundaries to be placed very close to the cavity for simulation. The thin-film oxide deposited by PECVD is a lossy material at terahertz frequencies. However, the accurate modeling of loss due to oxide is beyond the scope of this work, especially since the loss-parameters of the low-temperature ($\sim 100\,^{\circ}\mathrm{C}$) deposited oxide are not known.

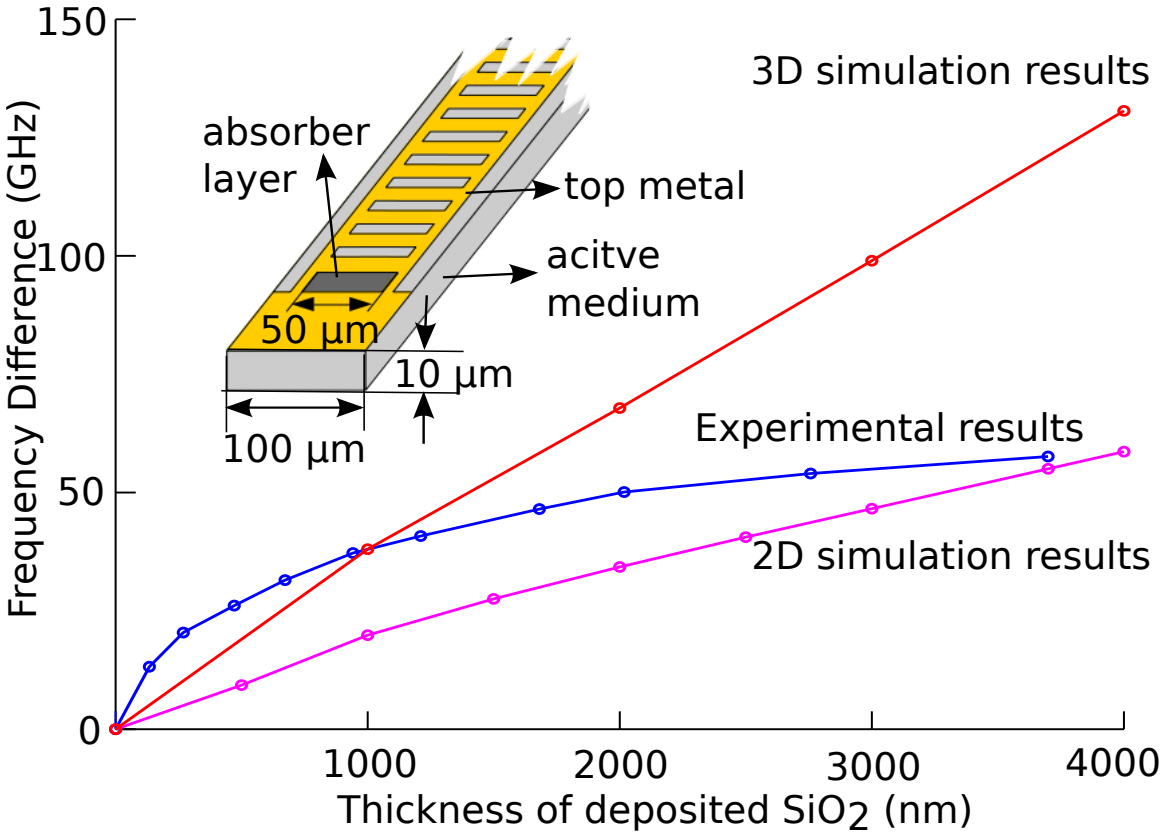

FIG. 7. **Frequency tuning versus deposited oxide thickness for the lowest-loss resonant-cavity mode for a QCL cavity with antenna-feedback scheme** Experimental tuning result for a 10 μm thick cavity is plotted alongside that obtained through 2D simulations (that models a cavity with infinite width), as well as results from full-wave 3D simulation in which the shown geometry is modeled for a cavity of 1.4 mm length.

To further explain the non-linear tuning performance, some 3D simulation results are also included in the Fig. 7. Considering the limitations in computer memory, the resolution of photolithography, and other uncertainties in fabrication (that include the curved sidewall profiles of the wet-etched cavities that is difficult to model), some simplifications are made in the creation of the geometry of 3D module. From the simulation results shown in Fig. S2, the tuning performance can be seen to vary significantly for 2D versus 3D simulation. It was also noticed that the simulated results were different if the 3D geometry was altered. Also, the effect of neighboring cavities cannot be captured in such a simulation due to lack of computer memory to simulate multiple cavities. Due to these reasons, any other simulations to estimate the non-linear tuning effect have proven to be futile.

It should also be noted that the large non-linear effect of tuning might also be attributed to some other reasons that may be difficult to model. One factor that may affect tuning

performance is the quality of the deposited oxide. Considering the Indium-solder mounted QCL chip in our experiments, a low deposition temperature ($\sim 100\,^{\circ}$C) was chosen for deposition, which resulted in poor quality of the deposited oxide. SEM images of the deposited SiO_2 show cracks on the surface of the SiO_2 (not shown here). The effect of oxide quality on tuning behavior is difficult to envision. However, we could safely conclude that the temperature performance of QCLs with deposited oxide could be improved if a better quality oxide can be deposited.

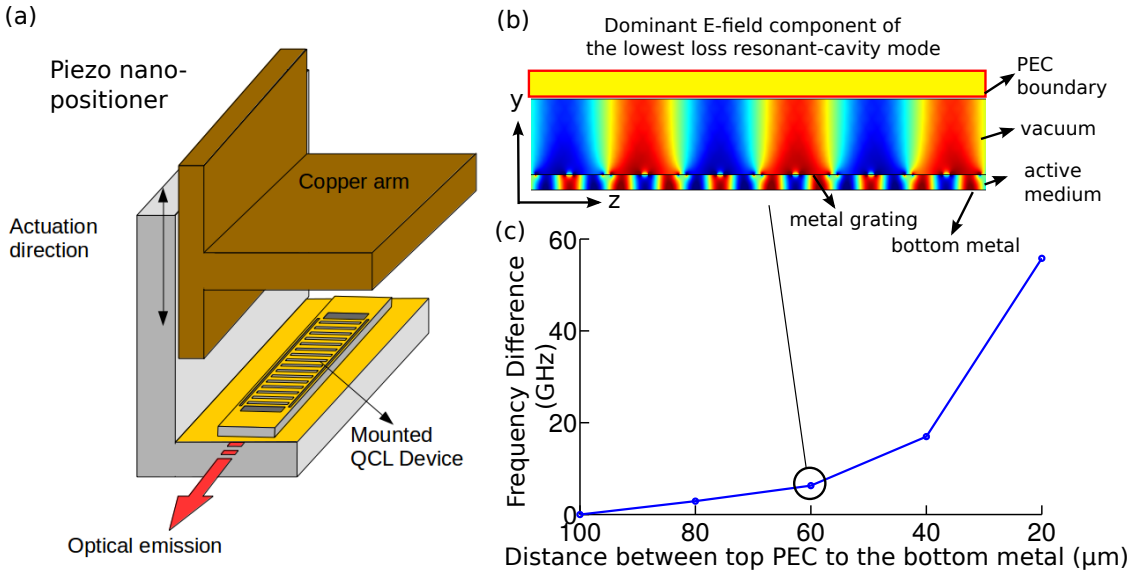

FIG. 8. **Illustration of a scheme to dynamically tune the resonant-cavity mode of a cavity with antenna-feedback scheme based on an electrically movable nano-positioner** (a) A possible dynamic tuning setup by using a metallic arm controlled by an piezo nano-positioner, located over the QCL cavity with antenna-feedback. (b) Mode-shape of the resonant-cavity mode with the metallic arm in vicinity of the cavity in the surrounding medium, modeled as perfect-electric-conductor in 2D finite- element simulations. (c) Frequency tuning results from the 2D simulation for the lowest-loss resonant-cavity mode, computed as a function of distance of the metallic arm from the bottom metallic plane of the cavity.

III. DYNAMIC TUNING BASED ON AN ELECTROMECHANICAL DEVICE

A relatively straightforward method to achieve dynamic tuning of terahertz QCLs with antenna-feedback scheme would be to utilize electromechanical nano-positioners, similar to those utilized for some terahertz QCLs in prior work as described in Refs. [22–24]. Thanks to the establishment of the strong hybrid SPP mode on the top of the cavity in vacuum, large

dynamic tuning is predicted based on simulations for such cavities with antenna-feedback scheme. The primary advantage of such a tuning scheme would be the capability to use wider cavities that will have a much better temperature performance, while still retaining narrow far-field radiation patterns are are a characteristic of the antenna-feedback scheme.

Fig. 8 illustrates a piezoelectric nano-positioner that could be utilized to control the distance between the laser cavity and an overhanging metallic arm attached to the nano-positioner. A 2D simulation was carried out to estimate the tuning performance for such an implementation. In this simulation, the metal arm was modeled as a perfect-electric-conductor (PEC) boundary. When the distance between the bottom metal of the laser cavity to the PEC boundary is changed from 100 μm to 40 μm, $\sim$ 17 GHz tuning is estimated for the resonant-cavity DFB mode. The SPP wave in the surrounding medium is considerably altered when the PEC boundary gets even closer and a large tuning of $\sim$ 60 GHz is predicted if the metallic arm could be brought to a distance of $\sim$ 20 μm from the ground plane, which should be realizable for piezo-based positioners with positioning accuracy of few microns.